# Impact angle and exposure time effects on raindrop erosion of fibre reinforced polymer composites: application to offshore wind turbine conditions

**Ghulam Rasool, Maria Pelaez Larios, Margaret M Stack**

Department of Mechanical and Aerospace Engineering

University of Strathclyde - James weir Building

75 Montrose Street

Glasgow G1 1XJ

United Kingdom

**Abstract**

Raindrop erosion significantly contributes to the leading edge erosion of rotor blades. The object of the current work is to investigate the causes of the leading edge erosion of a glass fibre reinforced polymer composite candidate wind turbine blade in condition of containing 3.5% NaCl, applicable to offshore wind turbine conditions or wind farms located close to coastal regions. For this purpose, a whirling arm rig was used to test specimens for a range of angles of attack at a constant tip speed of rotor blades. The tests were run for two hours and mass variation was measured after half hour interval. Scanning electron microscope (SEM) analyses of the exposed surfaces of each sample were carried out after the completion of tests. The test results reveal that droplet impact erosion of the rotor blade progresses in a so-called parabolic manner and the ingress of water and salt can affect the erosion resistance of the materials. Erosion maps have been constructed to demonstrate transitions in erosive wear modes with exposure time.

**Keywords:** Raindrop erosion, wind turbine blade, leading edge, erosion map

## 1 – Introduction

In order to increase the renewable energy share in the production of electricity, wind energy has a promising future. To develop the technology further and reduce energy generation cost to the level of other electricity-producing sources [1 - 3], one such approach is to tackle materials issues. One of the problems in the design of the structure is the selection of suitable structural materials for the wind turbine components, especially a durable, lightweight, high strength to density ratio and erosion resistant material for the large scale rotor blade.

The performance of a rotor blade is mainly affected by erosion damage on the leading-edge, which results in roughening of the aerofoil. Damage to this component results in up to 25% decrease in the coefficient of lift and a minimum of 60% increase in the coefficient of drag [4 - 6]. In order to generate higher megawatt energy outputs, designers and manufacturers have focused on a longer rotor blade. The tip speed of a bigger rotor blade increases significantly, which results in higher erosion on the blade due to raindrop erosion. The performance of eroded rotor blades can be reduced up to 25% depending upon the severity of the erosion degradation. Failure of the rotor blade is one of the most common and costly challenges, which the wind energy industry is currently addressing at the present as well as presenting environmental safety issues [7 - 15].

Raindrop erosion leads to pit formation, gouges, swelling of the matrix, de-bonding of the fibre-matrix interface, and exposure of the fibre, brittle fractures, and delamination. All these factors lead to damage at the leading and trailing edges of the rotor blade [16 - 22]. An eroded surface of the wind turbine blade can cause various issues including change in aerofoil shape, turbulent airflow over the blade, mass gain by diffusion, change in the coefficient of drag and coefficient of lift, unbalanced operation, and increased Reynolds number. All these factors affect the performance of the wind turbine significantly by an increase in failure rate; repair and operating cost, downtime, which result in reduced efficiency, availability, and reliability of the wind turbines [23, 24].

To address the above tribological issues, the material for the rotor blade must be lightweight, robust, have good mechanical properties, and erosion resistant to withstand the aggressive and potentially harsh environmental conditions. Fibre-reinforced polymeric composites have favourable mechanical and chemical properties and are being used in the manufacturing of wind turbine blades. The issue with these materials is their poor tribological resistant properties [16].

In order to address the above issues, in this work a G10 epoxy glass laminate polymer composite was tested for raindrop erosion under laboratory simulated offshore wind turbine blade operating conditions. The experiments were carried out in a whirling arm erosion test rig for two hours on each specimen in four intervals, i.e. 30 minutes each at a constant tip speed for the range of impact angles. The change in mass of the samples was

measured after every 30 minutes of the test run. After completion of each experiment, SEM analyses of the eroded surface were carried out to investigate the mechanisms of raindrop erosion progression with the exposure time. In the light of experimental results, an erosion map has been developed and included in this paper. This study will provide baseline data for the selection of erosion-resistant materials and coatings for the manufacturing of rotor blades. Moreover, a parabolic raindrop erosion progression trend on the leading edge of the wind turbine blade suggests that the selected material and coatings should have aim to extend the incubation period of the erosion process to complete its fault free service life.

## 2 - Experimental

### 2.1. Test rig

Figure 1(a) shows the whirling arm raindrop erosion test rig, which was used for this experimental work. This rig was constructed in the University of Strathclyde to replicate raindrop and wind turbine blade operation as per ASTM Standard MNL56-EB, Chapter 10-Erosion Testing [25]. In this arrangement, two arms rotate in a steel drum; each arm has a sample holder at one end to hold a specimen. The arms can be adjusted at the required angle of attack. The range of angles of attack that can be tested is 15 to 90° in an increment of 15°. Two samples can be tested at a time at different angles of attack. A ring is fixed above the trajectory of the specimen rotation to hold sixteen hypodermic needles fixed at the end of plastic tubes to replicate raindrops to impact rotating samples Fig. 1(b). A peristaltic pump supply rain solution through plastic tubes to produce droplets via needles Fig. 1(c). An electric motor rotates the sample holding arms like a rotor. Perspex tubes are provided around needles under the steel ring for the shielding of droplets from the interference of air and to make a proper impact on the specimen Fig. 1(b). The droplet size and frequency can be changed by adjusting the speed of the peristaltic pump Fig. 1(d). Various rotor blade tip speeds from 1 to 60 $ms^{-1}$ can be replicated for the testing purpose in this rig.

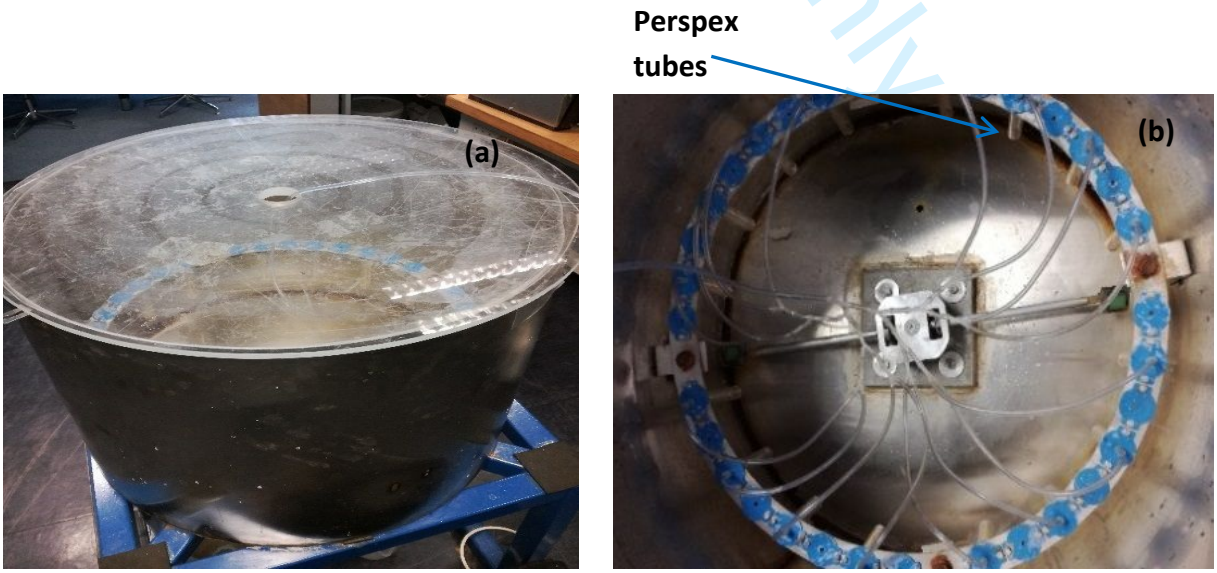

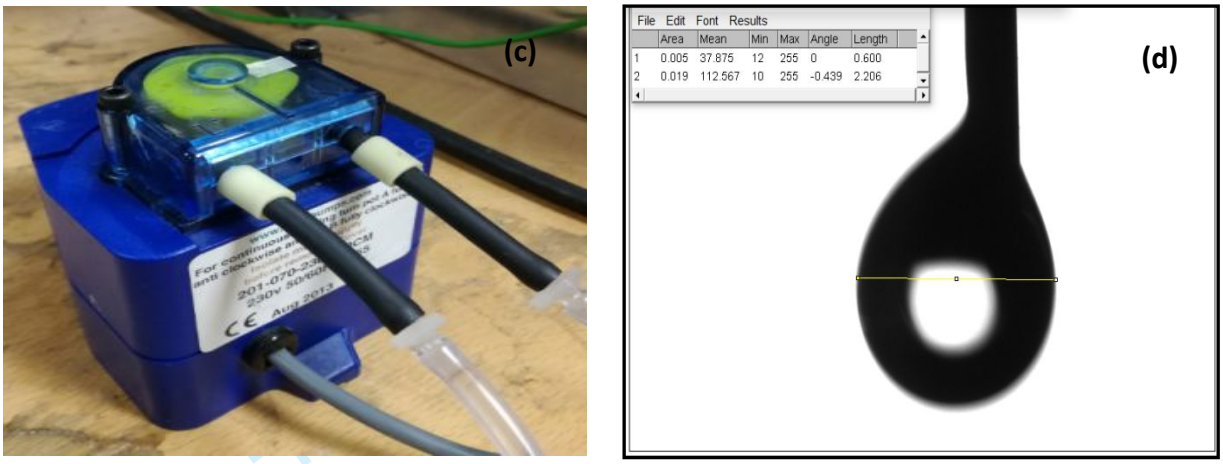


***Figure 1:*** *a) Whirling arms rig, b) whirling arms and raindrop arrangement, c) peristaltic pump to supply water, and d) droplet size.*

## 2.2. Materials

In the present research, a commercially available glass fibre reinforced polymer matrix composite (G10) was tested as an offshore wind turbine blade material Fig. 2. This composite is manufactured from continuous filament glass fibre cloth with epoxy as a resin binding agent. It is a thermoset, low moisture absorber, and highly noncorrosive material. This composite has a high strength to density ratio, high strength, high stiffness, and high creep resistance. This composite is already in use for several engineering applications in marine, aerospace, medical, energy, etc. industries. The physical and mechanical properties of this material are as below:

***Figure 2:*** *G10 epoxy glass laminate composite material sample.*

1 - Flexural strength (MPa) = 482

2 - Tensile strength (MPa) = 320

3 - Shear strength (MPa) = 131

4 - Chary impact strength (kJ $m^{-2}$) 65

5 - Density (g $cm^{-3}$) = 2

6 - Specific gravity = 2

7 - Water absorption (mg $m^{-2}$) = 8

8 - Hardness, Rockwell (m-scale) = 110

9 - Body colour = Green 10 - Standard finish = Satin/Glossy

2.3. Test conditions and procedure

Two hours experiment was run for each sample at each impact angle for the range of angles of attack 15° to 90° in an increment of 15°. Each experiment consists of four tests, i.e. of 30 minutes each on the same sample at each angle of attack. A tip speed 60 $ms^{-1}$ and drop size of 2.2 mm was kept constant for the whole series of tests. The rainwater solution was maintained at 3.5% of salt by the weight of water to replicate offshore conditions. After taking all safety measures and checks, the rig was calibrated for the required tip speed of the rotor blade and raindrop size. The test specimens were cut to the size 32 mm length and 30 mm width and finished from the sides with the fine sandpaper. Before the test starts each sample was weighed on an electronic balance accuracy of 0.01 mg. Two samples were tested at a time by holding and securing properly at the two arms end, which was positioned at the required angles of attack.

Prior to start of each test, the peristaltic pump was kept running about 10 minutes to ensure an equal supply and same size droplet coming from each of the sixteen needles. Subsequently, the electric motor was switched on to rotate the whirling arms at the constant speed, which was 60 $ms^{-1}$. After completion of 30 minutes test, the sample was rinsed in the simple water and left to dry at room temperature for 24 hours to minimise the absorption effect before the post-test weighing. After weighing, the same sample was tested for the next 30 minutes and so on till completion of two hours experiment. After completion of each test, the topography of the exposed surfaces was analysed by using high-resolution images advanced techniques, i.e. the scanning electron microscope (SEM) to establish raindrop erosion modes and mechanisms of this tribo-system.

**3 – Test results**

3.1. Erosion of the composite as a function of impact angles and exposure time.

**Table 1:** *Mass change trend at different impact angles for the successive test run times, (negative mass loss mean sample has gained mass).*

| Time (Minutes) | Mass loss ( x $10^{-4}$ g) at 15° | Mass loss ( x $10^{-4}$ g) at 30° | Mass loss ( x $10^{-4}$ g) at 45° | Mass loss (x $10^{-4}$ g) at 60° | Mass loss ( x $10^{-4}$ g) at 75° | Mass loss ( x $10^{-4}$ g) at 90° |
|---|---|---|---|---|---|---|
| 30 | 13.3 | 12.1 | 4.7 | 9.4 | 3.7 | 4.4 |
| 60 | -0.1 | 1.0 | -1.4 | -2.7 | -1.7 | -2.6 |
| 90 | 0.8 | 0 .2 | -3.2 | -2.1 | -1.7 | -4.3 |
| 120 | 5.9 | 5.2 | -0.8 | -1.7 | -1.0 | 0.3 |

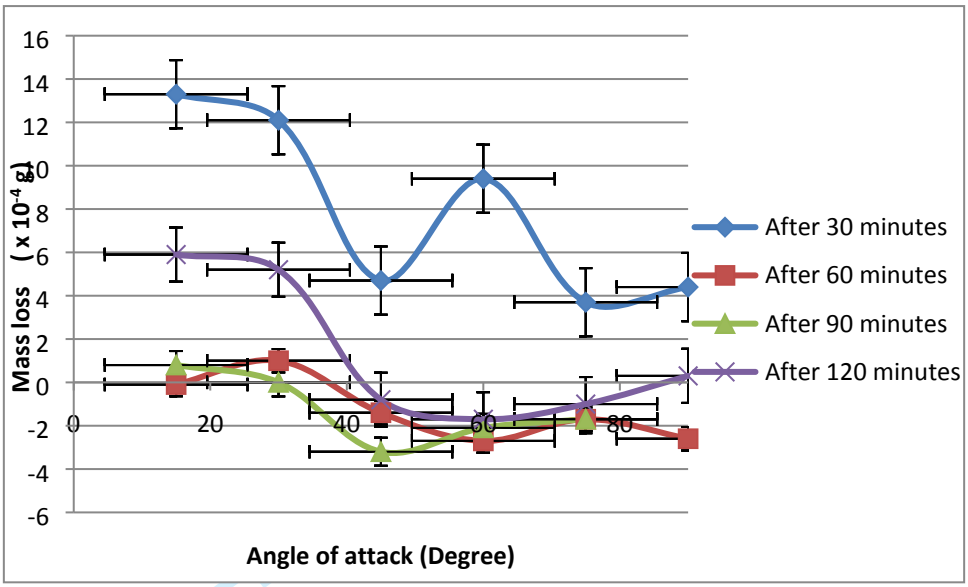


***Figure 3:*** *Mass change trend at different impact angles and test run durations.*

Table 1 and figure 3 shows a mass variation of the specimens at different angles of attack for different test intervals. The final mass after the completion of each 30 minutes interval varies for each combination of the angle of attack and experimental time. The graph shows that maximum mass loss occurred in the first 30-minute test duration for the range of angles of attack.

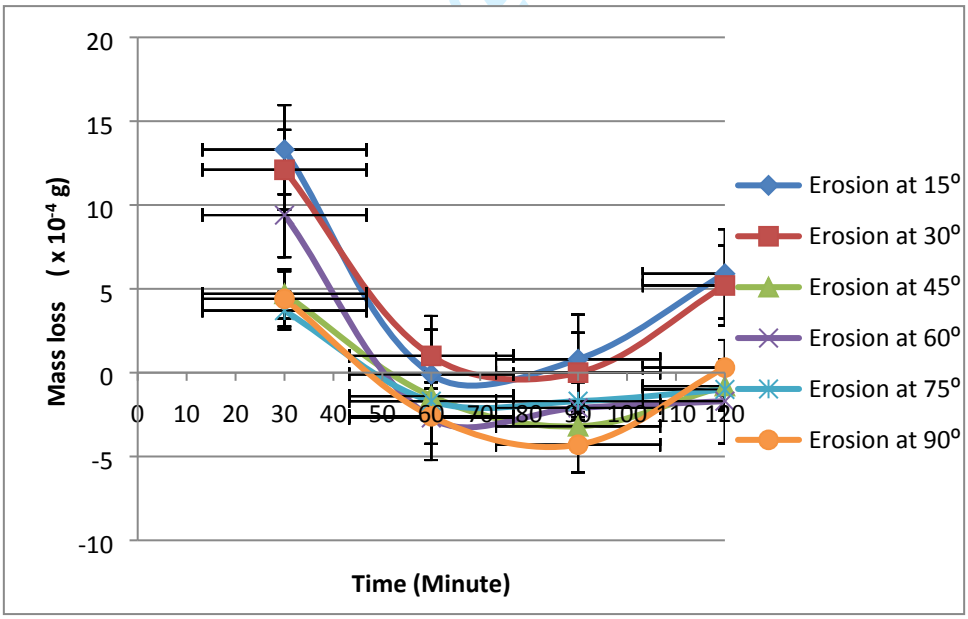


***Figure 4:*** *Successive erosion at different impact angles with respect to successive exposure times.*

Table 1 and figure 4 shows the successive erosive behaviour of the specimens for different test intervals at each angle of attack. A sharp decrease in the mass loss is apparent in the second run of tests, i.e. from 30 to 60 minutes. No apparent changes in mass variation in the third run, i.e. 60 to 90 minutes can be seen in this figure. All specimens show a mass gain in

the final test run, which is 90 to 120 minutes as the tests proceeded. This shows that the erosion due to raindrop impact on the leading edge of the rotor blade progress in a parabolic manner with an increase in exposure time. Moreover, the higher mass loss of this material due to erosion at lower angles of attack of the raindrop is dominating in this tribo system Fig. 3 & 4.

3.2. SEM images of the exposed surfaces.

Figure 5 shows SEM images of the exposed surfaces of each specimen after completion of the 2-hour test for the range of angles of attack. The impacts of raindrop have damaged exposed surfaces, which results in roughed topographies and mass loss of specimens. At the lower angles of attack, the shearing effects of the droplets due to outward spreading after impacting the target is deemed to be dominated. This spreading of the water occurs at very high speed, which results in excessive surface damaging and higher mass by matrix cutting, fractures, laminate delamination, debonding at skin/core interfaces, exposure and the buckling of the reinforced fibre of the exposed surface material Fig. 5 (a, b). With an increase in angle, a mixture of shearing and impact erosion mechanisms of droplets controls the damaging on the exposed surfaces. Swelling, fractures, pitting and gouges on the exposed surfaces along with pulled out matrix material is apparent for these impact angles Fig. 5 (c, d). At the higher angles of attack, the erosion of the specimens was dominated by the impact erosion of droplets Fig. 5 (e, f). The damaged surface of the specimens may help in the mass gain as well by the absorption of moisture and re-crystallization of salt in the cracks over the exposure time.

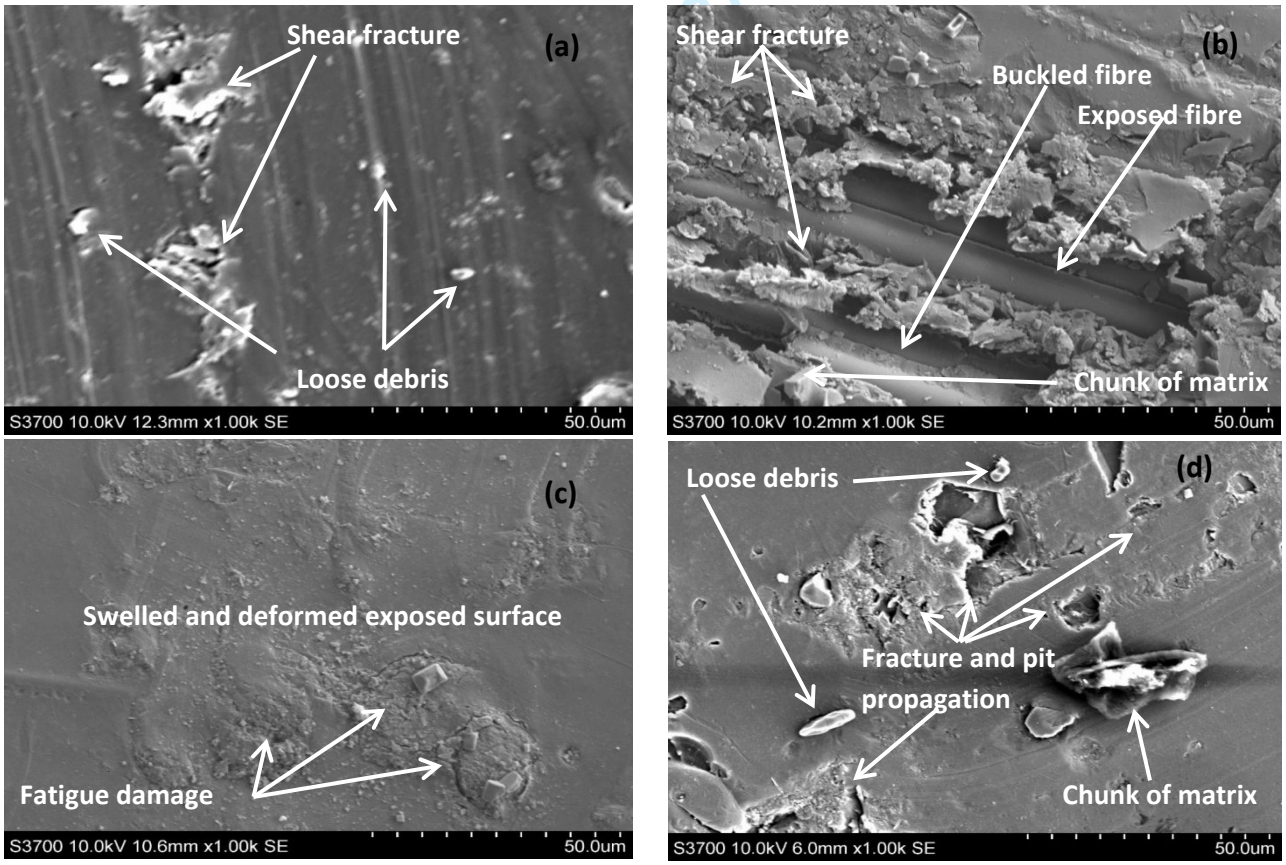

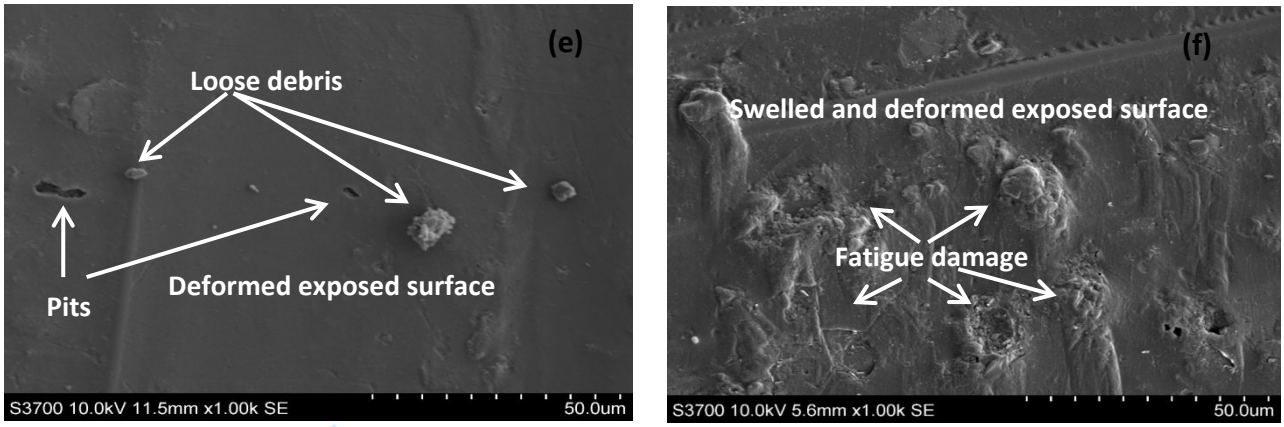


**Figure 5:** *SEM images of the exposed surfaces after completion of 2 hours test, a) at 15° impact angle, b) at 30°, c) at 45°, d) at 60°, e) at 75°, and f) at 90°.*

## 4 - Discussion

The erosion behaviour of materials is affected by the several factors including the material type, exposure conditions, mechanical properties, impact velocity, impact angle, and droplet size. The drag forces on wind turbines blade depend on the shape of an aerofoil, exposed surface roughness and tips speed of the blade. A maximum erosion of the rotor blade occurs on the leading edge, particularly towards the trailing edge where tip speeds are higher Fig. 6, [26]. The angle of attack depends on the shape of the aerofoil of a rotor blade. To extract the greatest power from the wind flow stream, the aerofoil of a rotor blade is designed for an angle of attack, which gives a higher value of the coefficient of lift to the coefficient of drag ratio. The erosion of rotor blades results in both the delamination of the leading edge material and the change in its shape, which result in a change in the coefficient of lift and coefficient of drag [17]. Moreover, roughening of the leading edge of the rotor blade leads to an increase in friction and Reynolds Number, which in turn results in an increased coefficient of drag.

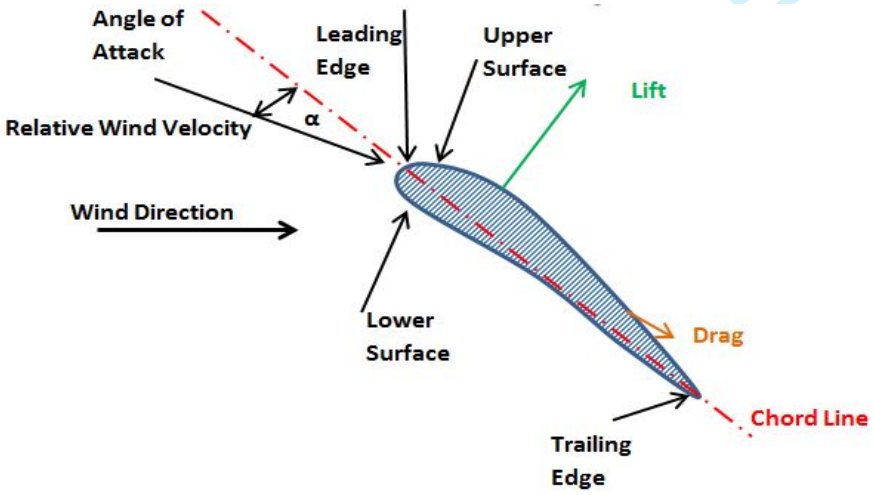

***Figure 6:*** *Schematic of angle of attack on the wind turbine blade leading edge.*

Several factors, such as wind speed, dust, polluted environment, rain, solid particle, insects, hailstone, icing, and sea spray that contributes to the progression of leading-edge erosion on the rotor blade. Out of these factors, raindrop erosion is a major contributor to this process at a higher tip speed of the blade [14, 15]. Raindrop erosion of the rotor blade progresses mainly in three stages, upper core and, lower core damage and leading-edge damages [27]. Furthermore, the erosion on the leading edge progresses in two ways, firstly, by the formation of a large number of pits and gouges near the leading edge and secondly on the lower surface of the blade since the raindrops impact at the positive angle of the attack on the rotor blade [28].

Due to the fact that it is an anisotropic material, the G10 epoxy glass laminate polymer composite is showing a semi-ductile erosion material behaviour. Fluctuation in the mass loss is evident from the test results for the range angles of attack Fig. 3. The erosion peak patterns of a higher mass loss at 30° for so called ductile materials and higher mass lass at 90° for so called brittle materials have not been followed by this composite Table 2, Fig. 3, [21, 29 - 31]. Contrary to that observed for solid particle erosion, the droplet erosion is controlled by the forces exerted by each droplet impact [32]. As soon as the droplet impacts the exposed surface a lateral water jet and Rayleigh wave is generated, which move through the blade material to shear it. The strength of this wave depends on the droplet size, angle of attack, and impact speed. These Rayleigh waves obtain the most of the energy generated by the impact of the droplet. Water spreading speed of the jet is at least three times higher than that of impact velocity [33]. Already existing cracks and defects in the surface material are more affected by the shear stress of the jetting [8, 34]. Continuous shearing action of the water jet and Rayleigh wave interactions produces stress on the exposed surface, which leads to damage and mass loss of the surface material by crack formation and erosion under fatigue [35 - 37].

Raindrop erosion process progresses into three stages, i.e. incubation period, increasing period, and steady state period. No noticeable mass loss occurs during the first stage because of limited deformation and restricted stress waves on the exposed surface. The material degradation is controlled by the droplet impact fatigue [20]. The erosion mass loss starts to occur as soon as the erosion process enters the increasing stage. Test results revealed that the G10 has a very short incubation period Fig. 4. The highest mass losses of this composite in the first interval, i.e. 0-30-minute test run are attributed to the combined action of water jetting and impact fatigue of the droplet. This interval of the experiment comprises the second stage of the erosion process, which led to roughening and shearing away of exposed surface materials to widen the cracks and shear failure [38, 39]. With an increase in exposure time cracks and pit propagation [17, 20, 40]; the delamination of the underlying layers of the composite occurred, which results in higher mass losses [17, 20, 40 - 43].

With the progression in experiments' time from 30 to 60 and 60 to 90-minutes, the erosion process entered to the so-called steady state period for the mass losses. The mass-loss rate of the specimens decreased sharply during along with mass gained at 60°, 75° and 90° angles of attack Fig. 3 and 4. The depth of the initially formed pits approached a specific point where the rate of pit deepening decreases. Moreover, as the depth of the pits increases, a protective water layer forms and remained over the exposed roughened surface. This layer acts as a squeeze layer damper for further droplet impact to damage, which results in a sharp decrease in the mass losses in these intervals of the experiment [17, 20, 44 - 46].

The mass gains in these intervals of the experiment at 60°, 75° and 90° angles of the attack were possibly caused by the damaged surface of this composite, which facilitates absorption of moisture by diffusion in the damaged areas. Moreover, the role of salt recrystallization in the cracks possibly also leads to a mass gain at the higher exposure time along with water absorption. This can contribute to the net decrease in mass losses [4, 16, 43]. The mass gain affects the mechanical properties and erosion behaviour of the blade material, which results in unexpected failure mechanisms of the blade materials. Therefore, it is essential to explore thoroughly effects of water absorption and exposure time on the progression of the erosion mechanisms of the rotor blade to mitigate this problem [47].

With an increase in the exposure period, i.e. 90 to 120 minutes of the test run, there are mass losses of all specimens Fig. 4. The higher mass losses trend at 15° and 30° angles of attack is being maintained throughout the experiment Fig. 3 and 4. Moreover, the erosion progression curves have taken parabolic shapes Fig. 4. With the progression of the experiment, fatigue is accumulated on the exposed surface. Both the raindrop impact forces and fatigue erosion result in damage of the exposed surface. The literature shows that the erosion induced damages and raindrop impact forces induced damages occurred by the cube power and square power of the tip speed respectively, which result in severe damage of the exposed surface and higher mass losses [14, 48, 49]. A parabolic progression in erosion with an exposure time after the incubation period is attributed to the combined action of raindrop impact, fatigue, and change in mechanical properties of the blade material [44, 48].

Raindrop erosion on a wind turbine blade is a continuous phenomenon of degradation of blade material [50], which progresses by pit formation, gouging, swelling, de-bonding of the fibre-matrix interface, exposed fibre, brittle fractures, chunking, and delamination of the exposed surfaces Fig. 5. The impact angle and tip speed play an important role in the erosion mechanisms and degradation of the material. At lower impact angles, the erosion of exposed surfaces seems to be controlled by the shearing effects of the droplet. The chunking leads to exposing the reinforced fibre. Eventually, impact and shearing forces of the droplet directly affect fibre to buckle, fracture, and remove it from the matrix Fig. 5 (a, b, c). At higher angles of attack, erosion is dominated by droplet impact damages, i.e. compressive high-pressure regime Fig. 5 (d, e, f). Semi-ductile erosion behaviour of this

composite is clear for both lower angles of attack Fig. 5 (a, b, c), and for the higher Fig. 5 (d, e, f). The topographies of the eroded surfaces, Fig. 5, are in line with the mass loss results in Fig. 3 & 4 and research work found in the literature [4, 16, 51 - 53].

4.1. Erosion progression map

An erosion map is one of the design analysis tools which investigates and predicts modes and regimes of degradation of a rotor blade material. This map demonstrates the level of degradation, wastage, and the extent of safe working conditions for the rotor blade material. In the light of experimental results, an erosion map has been constructed to predict the progression in degradation on the leading edge of the wind turbine blade Fig. 7. The erosion modes are termed as mass loss + surface damage, surface damage, surface damage + mass loss with the domination of erosion mechanisms in this test window. The erosion modes regime and modes transitions boundaries are approximate and drawn by considering mass variation trends during the experiments and post-test eroded surface topography analyses by SEM Table 1 and Fig. 3, 4, and 5.

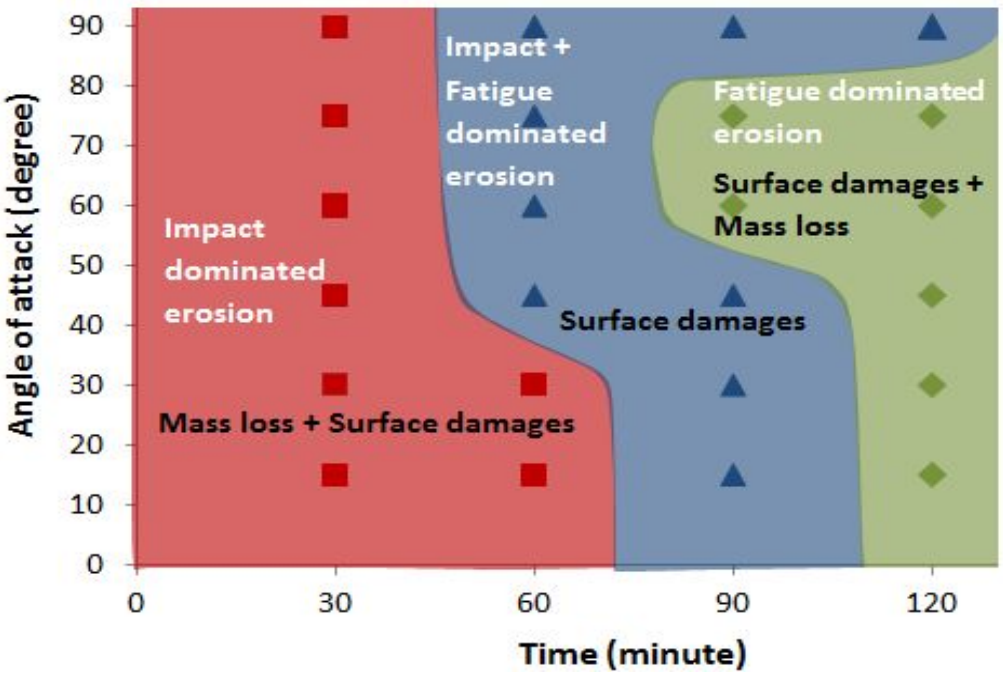


**Figure 7:** The wind turbine blade leading edge erosion progression map.

In this map, the mass loss + surface damage zone shows the erosion is dominated by the impact of the droplet which results in a higher mass loss by pit formation and buckling of the matrix material. With the progression in the exposed period, erosion mode transition occurs from mass loss to surface damages dominated with sharp decreases in mass losses. The erosion is controlled by the combined effect of impact and fatigue under the repeated impact of droplets. With further increase in exposure period, mass loss started to increase,

which results in a parabolic transition of erosion regime from surface damages to surface damages + mass loss under fatigue dominated erosion.

To continue our research for the selection of proper erosion-resistant material and coating for the manufacturing of wind turbine blade, G10 epoxy glass laminate was tested in a wind turbine laboratory simulated conditions. In the light of the above investigation, an uncoated fibre reinforced polymer composite wind turbine blade, such as G10 has very poor raindrop erosion resistance in spite of its good mechanical properties. This work aids in understanding the raindrop erosion modes progression and transitions on the leading edge of the wind turbine rotor blade. Future work will evaluate coatings in such conditions in order to optimize material performance.

**5 – Conclusions**

1. The progression in raindrop erosion on the leading edge of the wind turbine blade of G10 epoxy glass laminate composite was investigated in laboratory simulated conditions. This uncoated material has shown relatively poor tribological resistance for the wind turbine rotor blade applications.

2. The erosion process initially starts from the pit formation near the leading edge, which extends to gouges, fractures, cracks, and finally wastage of material from the exposed surface by delamination and chunking under fatigue.

3. The depth of the pit and damping effect of the water layer on the roughened surface results in a sharp decrease in material loss by erosion.

4. The ingress of salt over a period of time together with swelling of polymer material may lead to weight gain and surface roughening thereby changing the aerodynamics and ultimately the efficiency of the turbine blade.

5. Leading-edge erosion resistance of the wind turbine blades may be enhanced by surface treatment techniques, such as application of hybrid composite coatings on the rotor blades. Future work will be evaluating the erosion behaviour of various erosion resistant coatings in such conditions.

**Acknowledgements**

The authors would like to acknowledge the support of the Interreg (Northern Ireland – Ireland – Scotland) Special EU Programmes Grant No SPIRE2_INT – VA – 049 ‘‘Storage Platform for the Integration of Renewable Energy (SPIRE 2)’’.

## References:

[1] https://www.lse.ac.uk/GranthamInstitute/faqs/what-are-the-pros-and-cons-of-onshore-wind-energy.

[2] Gervois, G., Offshore LNG Receiving Terminals: An Alternative To Onshore Terminal. Offshore Mediterranean Conference and Exhibition, 2007, Issue OMC-2007-142.

[3] https://www.nesgt.com/blog/2016/07/offshore-and-onshore-wind-farms.

[4] Kieran Pugh, Ghulam Rasool, Margret M Stack, Some thoughts on mapping tribological issues of wind turbine blades due to effects of onshore and offshore raindrop erosion, J Bio and Tribo-Corrosion (2018) 4: 50. https://doi.org/10.1007/s40735-018-0165-9.

[5] J. M. Janiszewska, R. Reuss Ramsay, M. J. Hoffmann, G. M. Gregorek, Effects of Grit Roughness and Pitch Oscillations on the S814 Airfoil; Technical Report; NREL/TP-442-8161; National Renewable Energy Laboratory: Golden, CO, USA, 1996.

[6] M. Schramm, H. Rahimi, B. Stoevesandt, and K. Tangager, The Influence of Eroded Blades on Wind Turbine Performance Using Numerical Simulations, Energies (MDPI), Received: 23 August 2017; Accepted: 11 September 2017; Published: 16 September 2017.

[7] M. H. Keegan, D. H. Nash, M. M. Stack, Modelling rain drop impact on offshore wind turbine blades, In: ASME Turbo Expo 11- 15 June 2012.

[8] J. Liersch and J. Michael, Investigation of the impact of rain and particle erosion on rotor blade aerodynamics with an erosion test facility to enhancing the rotor blade performance and durability, Journal of Physics: Conference Series 524 (2014) 012023 doi:10.1088/1742-6596/524/1/012023.

[9] M. H. Keegan, D H Nash, M M Stack, Topical Review: On erosion issues associated with the leading edge of wind turbine blades, Journal of Physics D: Applied Physics, 46 (38), ISSN 0022-3727, http://dx.doi.org.10.1088/0022-3727/46/38/383001.

[10] A. Corsini, A. Castorrini, E. More, F. Rispoli, F. Sciulli, P. Venturini, Modelling of raindrop erosion in a multi-MW wind turbine, Proceeding of ASME Turbo Expo 2015: Turbine Technical Conference and Exposition GT2015, June 15-19, 2015, Montreal, Canada.

[11] F. M. Larsen and T. Sorensen, New lightning qualification test procedure for large wind turbine blades, proceeding of the international conference on lightning and static electricity, Blackpool, 16-19 September 2003.

[12] http://environmentalresearchweb.org/cws/article/opinion/37719.

[13] C. C. Ciang, J. R. Lee, and H. J. Bang, Structural health monitoring for a wind turbine system: A review of damage detection methods, Measurement Science and Technology, Vol. 19 (2008): 122001.

[14] G. Fiore, and M. S. Selig, “A Simulation of Operational Damage for Wind Turbines,” Proceedings of the 32nd AIAA Applied Aerodynamics Conference, AIAA Paper 2014–2848, Atlanta, GA, 2014.

[15] G. Fiore, G. E. C. Fujiwara, and M. S. Selig, “A Damage Assessment for Wind Turbine Blades from Heavy Atmospheric Particles,” Proceedings of the AIAA Conference, AIAA Paper 2015–1495, Kissimmee, FL, 2015.

[16] G. Rasool, Shayan Sharifi, Cameron Johnstone, and Margaret M. Stack, Mapping synergy of erosion mechanisms of tidal turbine composite materials in sea water conditions, Journal of Bio- and Tribo-Corrosion, DOI: 10.1007/s40735-016-0040-5, June 2016, 2:13.

[17] G. Olive Angel, Mechanism of rain erosion Part 2. A critical review of erosion by water drop impact, WADC Technical Report 1953-192 Part 2.

[18] G. Hoff, W. Herbert, and H. Rieger, Rain and sand erosion, Phenomena of material destruction caused by repeated loads, Characterisation and determination of erosion resistance, ASTM STP 474, American Society for Testing and Materials, 1970, pp. 353-382.

[19] A. F. Conn and S. L. Ruddy, Effect of fatigue and dynamic recovery on rain erosion, Erosion, wear and interfaces with corrosion, ASTM 567, American Society of Testing and Materials, 1974, pp. 239-269.

[20] S. George Springer and I. Yang Cheng, Model for rain erosion of fibre reinforced composites, AIAA Journal, Vol. 13. No. 7, July 1975.

[21] F. George, Jr. Schmitt, Liquid and solid particle impact erosion, Coating and thermal protection materials branch non-metallic material division, Technical report AFML-TR-79-4122, November 1979.

[22] A. O'Carroll, M. Hardiman, E. F. Tobin, T. M. Young, Correlation of the rain erosion performance of polymers to mechanical and surface properties measured using nanoindentation, Wear 412-413 (2018), pp. 38-48.

[23] M. D. Reder, E. Gongzalez, J. J. Melero, Wind turbine failures – Tackling current problems in failure data analysis, Journal of Physics: Conference Series 753 (2016) 072027.

[24] N. Gaudern, A practical study of the aerodynamic impact of wind turbine blade leading edge erosion, 2014 J. Phys.: Conf. Ser. 524 012031.

[25] G. Kenneth (West Conshohocken, PA: ASTM International, 2007), 86-94, "Chapter 10-Erosion Testing," in Guide to Friction, Wear, and Erosion Testing, https://doi.org/10.1520/MNL11350M.

[26] Leon Mishnaevsky Jr. * ID , Kim Branner, Helga Nørgaard Petersen, Justine Beauson, Malcolm McGugan and Bent F. Sørensen, Review Materials for Wind Turbine Blades: An Overview, Materials, Published: 9 November 2017.

[27] G. Fiore, and S. Selig Michael, Simulation of damage progression on wind turbine blades subject to particle erosion, AIAA SciTech, 4-8 January 2016, San Diego, California, 5th AIAA Aerospace Science Meeting.

[28] A. Sareen, C. Sapre, M. Selig, Effects of leading edge erosion on wind turbine blade performance, Wind Energy, 2014, 17 (10), pp. 1531-1542.

[29] Tamer Sinmazcelik, Isa Taskiran, Erosive wear behaviour of polyphenylenesulphide (PPS) composites, Materials and Design 28 (2007) 2471-2477.

[30] N. M. Barkoula, J. Karger-Kocsis, Effects of fibre content and relative fibre orientation on the solid particle erosion of GF/PP composites, Wear 252, (2002), Pages 80-87.

[31] A. Helle, P. Andersson, T. Ahlroos, V. Kupiainen, Erosive wears of coatings and methods to monitor coating wear – A literature study, RESEARCH REPORT NO BTUO43- 041265 29.9.2004.

[32] M. Ku Lee, W. Whoe Kim, C. Kyu Rhee, W. Jong Lee, Liquid impact erosion mechanism and theoretical impact stress analysis in TiN-coated steam turbine blade materials, Metallurgical and Materials Transaction, April 1999, Volume 30, Issue 4, pp. 961–968.

[33] F. P. Bowden, The formation of micro jets in liquid under the influence of impact of shock, Philos. Trans. R. Soc. A 260 (1110), 1966, pp. 94-95.

[34] N.-M. Barkoula, J. Karger-Kocsis, Review Processes and influencing parameters of the solid particle erosion of polymers and their composites, Journal of materials Science, September 2002, Volume 37, Issue 18, pp. 3807–3820.

[35] J. E. Field, S. van der Zwaag, D. Townsend, J. P. Dear, Liquid impact erosion mechanisms in transparent materials, Physics and Chemistry of Solids, Cavendish Laboratory, Madingley Road, Cambridge, C83 0HE, UK, Final Report for Period 30th September 1980 to March 1983.

[36] F. P. Bowden, *and J. F. Field,* The Brittle Fracture of Solids by Liquid Impact, by Solid Impact, and by Shock *Proc*. *Roy*. *Soc*. *London, A282*; *331,* (*1964*).

[37] O. Gohardani, Impact of erosion testing aspects on current and future flight conditions, Prog. Aerosp. Sci. 47(2011), pp 280–303.

[38] E. F. Tobin, T. M. Young, Analysis of incubation period versus surface topographical parameters in liquid droplet erosion tests, ASTM Spec., Ed. 6 (2) (2017), pp. 144-164.

[39] F. P. Bowden, J. H. Brunton, the deformation of solids by liquid impact at supersonic speed, Proc. R. Soc., A 263(1315) (1961), pp.433-450.

[40] F. J. Heymann, Erosion by liquid … the mysterious murder of metals, Mach. Des. (1970), pp. 118-124.

[41] K. Wood, Blade repair: closing the maintenance gap, Composite world,

https://www.compositesworld.com/articles/blade-repair-closing-the-maintenance-gap.

[42] H. Masato, Cavitation damages mechanism and its correlation to physical properties of material, Characterisation and determination of erosion resistance, ASTM STP 474, American Society for Testing and Materials, 1970, pp. 48-66.

[43] G. H. Jilbert, J. E. Field, Synergistic effects of rain and sand erosion, Wear 243 (1), pp. 6-17.

[44] B. Amirzadeh, A. Louhghalam, M. Raessi, M. Tootkaboni, A computational frame work for the analysis of rain-induced erosion in wind turbine blades, Part I, Stochastic rain texture model and drop impact simulations, Journal of Wind Engineering and Industrial Aerodynamics, 163 (2017), pp. 33-43.

[45] C. M. Preece, N. H. Macmillan, Erosion Annual Review, Material Science, 7(1), 1977, pp. 95-121.

[46] G. P. Thomas, J. H. Brunton, Drop impingement erosion of materials, Proc. R. Soc. London, A. Math. Physic Sci., 314 (1519), 1970, pp. 549-565.

[47] P. Daviesa, * , G. Germainb , B. Gaurierb , A. Boisseaua , D. Perreuxc**,** Evaluation of the durability of composite tidal turbine blades, Proceedings of the royal society of London (A) February 2013, Volume 371 (1985), Pages 1-15 http://dx.doi.org/10.1098/rsta.2012.0187.

[48] B. Amirzadeh, A. Louhghalam, M. Raessi, M. Tootkaboni, A computational frame work for the analysis of rain-induced erosion in wind turbine blades, Part II, Drop impact-induced stresses and blade coating fatigue life, Journal of Wind Engineering and Industrial Aerodynamics, 163 (2017), pp. 44-54.

[49] G. Fiore, and M. S. Selig, Simulation of Damage progression on wind turbine blades subject to particle erosions, AIAA SciTech, 4-8 January 2016, San Diego, California, 54th. AIAA Aerospace Science Meeting.

[50] ASTM G40-99, Standard terminology relating to wear and erosion, ASTM International, 1999, p 12.

[51] T. Peterson, "Multiple Water Drop Impact Damage in Layered Infrared Transparent Materials," Erosion: Prevention and Useful Applications, STP664-EB, Adler, W., Ed., ASTM International, West Conshohocken, PA, 1979, pp. 279-297, https://doi.org/10.1520/STP35805S**.**

[52] W. F. Adler, The mechanics of liquid impact, Treatise on materials science and technology, Materials-Erosion, Academic Press 1979.

[53] S. S. Cook, Erosion by water-hammer. *Proc*. Roy. *Soc*. *London A119*: *481*, (*1928*).